Discovery and Characterization of a Group of Fungal Polycyclic Polyketide Prenyltransferases

Yit-Heng Chooi,*,[†] Peng Wang,[†] Jinxu Fang,[§] Yanran Li,[†] Katherine Wu,[†] Pin Wang,[§] and Yi Tang*,[†,‡]

[†]Department of Chemical and Biomolecular Engineering and [‡]Department of Chemistry and Biochemistry, University of California, Los Angeles, California 90095, United States

[§]Department of Chemical Engineering and Materials Science, University of Southern California, Los Angeles, California 90089, United States

S *Supporting Information*

ABSTRACT: The prenyltransferase (PTase) gene *vrtC* was proposed to be involved in viridicatumtoxin (**1**) biosynthesis in *Penicillium aethiopicum*. Targeted gene deletion and reconstitution of recombinant VrtC activity in vitro established that VrtC is a geranyl transferase that catalyzes a regiospecific Friedel−Crafts alkylation of the naphthacenedione carboxamide intermediate **2** at carbon 6 with geranyl diphosphate. VrtC can function in the absence of divalent ions and can utilize similar naphthacenedione substrates, such as the acetyl-primed TAN-1612 (**4**). Genome mining using the VrtC protein sequence leads to the identification of a homologous group of PTase genes in the genomes of human and animal-associated fungi. Three enzymes encoded by this new subgroup of PTase genes from *Neosartorya fischeri*, *Microsporum canis*, and *Trichophyton tonsurans* were shown to be able to catalyze transfer of dimethylallyl to several tetracyclic naphthacenedione substrates in vitro. In total, seven C_5- or C_{10}-prenylated naphthacenedione compounds were generated. The regioselectivity of these new polycyclic PTases (pcPTases) was confirmed by characterization of product **9** obtained from biotransformation of **4** in *Escherichia coli* expressing the *N. fischeri* pcPTase gene. The discovery of this new subgroup of PTases extends our enzymatic tools for modifying polycyclic compounds and enables genome mining of new prenylated polyketides.
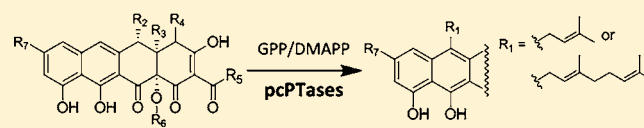
INTRODUCTION

Prenylation of aromatic compounds is a common biosynthetic strategy that contributes to the structural diversity of natural products. Many prenylated natural products are known to possess interesting biological activities, which include the anti-cancer tryprostatins (anti-tubulin and breast cancer resistance protein inhibitor),[1,2] the aminocoumarin antibiotics (bacterial DNA gyrase inhibitor),[3] the immunosuppressive drug mycophenolic acid (inosine-5′-monophosphate dehydrogenase inhibitor),[4] the anti-inflammatory panepoxydone (NF-κB inhibitor),[5] and many prenylated plant flavonoids.[6] Aromatic prenyltransferases (PTases), which catalyze the Friedel−Crafts alkylation of aromatic compounds with isoprenoid substrates, play a critical role in the biosynthesis of these structurally diverse molecules. The prenyl group of these compounds can contribute significantly to the known pharmacological activities, as demonstrated for apigenin and liquiritigenins[7] and tryprostatins.[8] Installation of prenyl chains results in increased lipophilicity of the compounds and enhances their interactions with biological membranes and proteins.[6] Therefore, the potential application of PTases as a medicinal chemistry tool to introduce isoprenoid substitution in different scaffolds has generated much research into various aromatic PTases from bacteria and fungi.[9,10]

Indole PTases are the most common aromatic PTases found in fungi. Many members of this family of enzymes are known to catalyze prenyl transfer to tryptophan or indole derivatives; thus, they are also referred to as dimethylallyltryptophan synthases (DMATS)-type PTases. The DMATS-type PTases are soluble, non-membrane-bound, and metal ion-independent enzymes and exhibit no significant sequence similarities to the *trans*-PTases in the biosynthesis of terpenoids, the membrane-bound aromatic PTases, and the soluble ABBA aromatic PTases (ABBA referring to the *αββα* structural motif) from bacteria.[10,11] In contrast to the bacterial ABBA PTases, which have been shown to catalyze prenyl transfer reaction to phenylpropanoids, flavonoids, and dihydroxynaphthalenes,[12] most characterized fungal DMATS-type PTases act on indole/tryptophan derivatives or, in an isolated case, a tyrosine, and only accept dimethylallyl diphosphate (DMAPP) as the prenyl donor.[10,13] In the X-ray structure, FgaPT2, a DMATS-type PTase from *Aspergillus fumigatus* involved in biosynthesis of ergot alkaloids, was shown to contain a barrel fold similar to bacterial ABBA PTases, but they differ significantly in the primary sequence and may only be distantly related evolutionarily.[14]

Viridicatumtoxin **1** is a polyketide-isoprenoid hybrid natural product isolated from *Penicillium aethiopicum* IBT 5753 (Scheme 1). **1** consists of a tetracyclic scaffold of polyketide origin and a geranyl-derived spirobicyclic ring that bridges the D and C rings of the naphthacenedione. **1** has been shown to

Scheme 1. Fungal Tetracyclic Compounds Compared to the Structure of Anhydrotetracycline from Bacteria
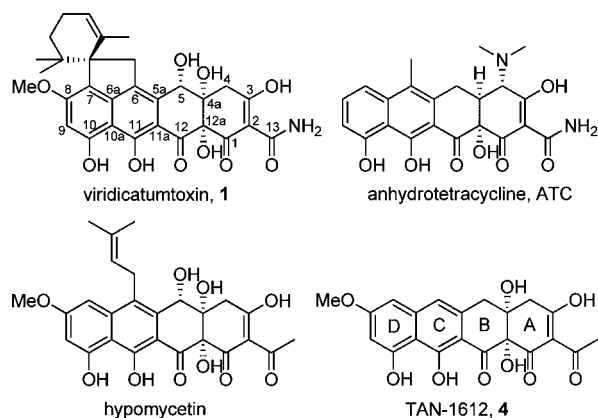
be nephrotoxic to rats and exhibits modest anti-tumor activity.[15,16] Anti-bacterial activity against methicillin-resistant *Staphylococcus aureus* has also been reported for **1** along with an epoxide derivative, viridicatumtoxin B, isolated from *Penicillium* sp. FR11.[17] The *vrt* gene cluster for biosynthesis of **1** was discovered via whole genome sequencing of *P. aethiopicum* IBT 5753 and confirmed by deletion of the core PKS gene *vrtA*.[18] Biosynthesis of the tetracycline-like naphthacenedione scaffold has been uncovered in our recent study, where three genes, encoding for a non-reducing polyketide synthase (NRPKS, VrtA), a β-lactamase-type thioesterase (MβL-TE, VrtG), and a flavin-dependent monooxygenase (FMO, VrtH), are shown to be essential for the formation of the tetracyclic structure.[19]

The geranyl-derived spirobicyclic ring of **1** was proposed to be introduced by a PTase VrtC (25% identity to known DMATS-type PTases) to C6 of the naphthacenedione **2**, followed by cyclization of the geranyl moiety to form the final spirobicyclic ring in **1** (Scheme 2). Until the recent discovery of XptA and XptB in *Aspergillus nidulans*,[20] VrtC was the only fungal DMATS-type PTase that had been linked to a polyketide–isoprenoid hybrid natural product. The DMATS-type PTases XptA and XptB were shown to be responsible for the biosynthesis of prenylated xanthones in *A. nidulans* via gene deletion studies.[20] VrtC is unique, as it may utilize a tetracyclic naphthacenedione substrate (Scheme 2), which is structurally similar to anhydrotetracycline (ATC), the key precursor of tetracycline antibiotics (Scheme 1). Dimethylallyl substitution of a naphthacenedione core is similarly anticipated in the biosynthesis of hypomycetin, an anti-fungal compound isolated from *Hypomyces aurantius* that is structurally related to **1** (Scheme 1).[21] The discovery and characterization of these

polyketide-modifying PTases in fungi indicate that DMATS-type PTases may catalyze the prenylation of a wider range of substrates than previously perceived, and that there may be more such enzymes to be discovered.

Here, we provide genetic evidence for the involvement of *vrtC* and *vrtD* (a putative geranyl diphosphate synthase gene) in the biosynthesis of **1**. VrtC was expressed in *Escherichia coli*, and its activity was reconstituted in vitro. Genome mining with VrtC protein sequences led to the discovery of a new group of polycyclic PTases distributed among fungi known to associate with human and animal diseases.

■ RESULTS

Targeted Deletions of *vrtC* and *vrtD* and Identification of Intermediates 2 and 3. The PTase encoded by *vrtC* was proposed to function as a geranyl transferase in biosynthesis of **1**.[18] On the other hand, *vrtD* is likely to encode for a geranyl diphosphate synthase (GPPS) due to its similarity to other farnesyl pyrophosphate synthases (FPPSs) (Scheme 2). Fungal terpene cyclases are known to exhibit structural homology to FPPSs,[22] hence VrtD may also be responsible for the cyclization of the geranyl moiety into the spirobicyclic ring in **1**, since no other cyclase was found in the *vrt* cluster. To verify the function of these two genes, we performed targeted gene deletions by double homologous gene replacement with the *bar* (glufosinate resistance gene) cassette on the *P. aethiopicum* Δ*gsfA::zeo^R* strain (Figure S1). The *P. aethiopicum* Δ*gsfA::zeo^R* was generated in a previous study to remove the high-yielding griseofulvin metabolite, which interferes with analysis of other metabolites present at lower titers.[23] Glufosinate-resistant transformants were successfully obtained and the Δ*vrtC* mutants were screened by diagnostic PCR (Figure S1). Three-day cultures of Δ*gsfA*/Δ*vrtC* mutants grown in glucose minimal medium (GMM) were extracted with organic solvent, dried, and subjected to metabolite analysis by liquid chromatography–mass spectrometry (LC/MS). As expected, deletion of *vrtC* abolished the production of **1** and led to the accumulation of a non-geranylated tetracyclic product **2** with *m/z* 414 $[M+H-H_2O]^+$ and 432 $[M+H]^+$ (Figure 1 and Table S3). The structure of **2** was solved by ^1H, ^{13}C, and 2D NMR (Table S3) and was shown to be 5-hydroxyanthrotainin, which has an additional hydroxyl group at the C5 position compared to the substance P antagonist anthrotainin from *Gliocladium catenulatum*.[24]

Besides loss of **1** and accumulation of **2**, a peak (**3**) with *m/z* 550 $[M+H-H_2O]^+$ and 568 $[M+H]^+$ (Table S4), which is present in small amount in both wild-type and Δ*gsfA P. aethiopicum* strains, was also abolished in the *P. aethiopicum*

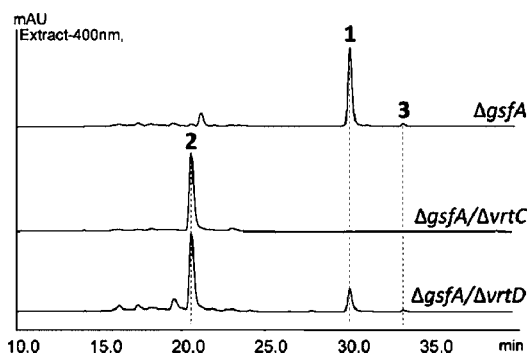## Scheme 2. Regiospecific Prenylation of 2 by VrtC Using the Geranyl Diphosphate Substrate
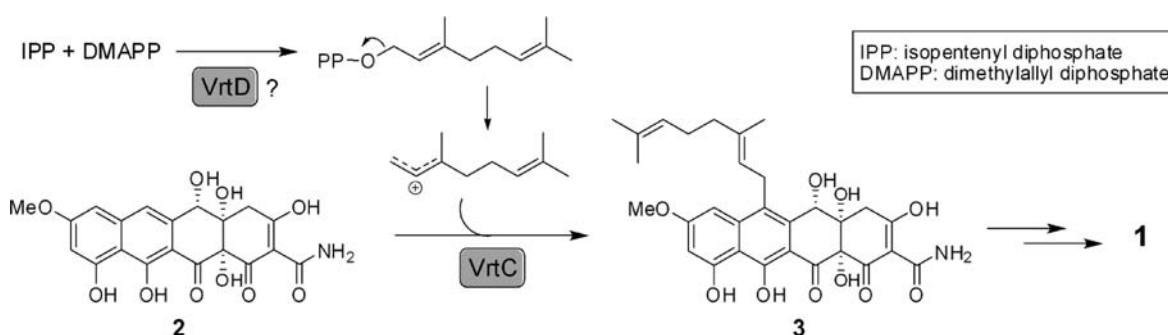
Figure 1. Changes in the metabolic profiles resulting from deletion of *vrtC* and *vrtD* in *P. aethiopicum* Δ*gsfA*.
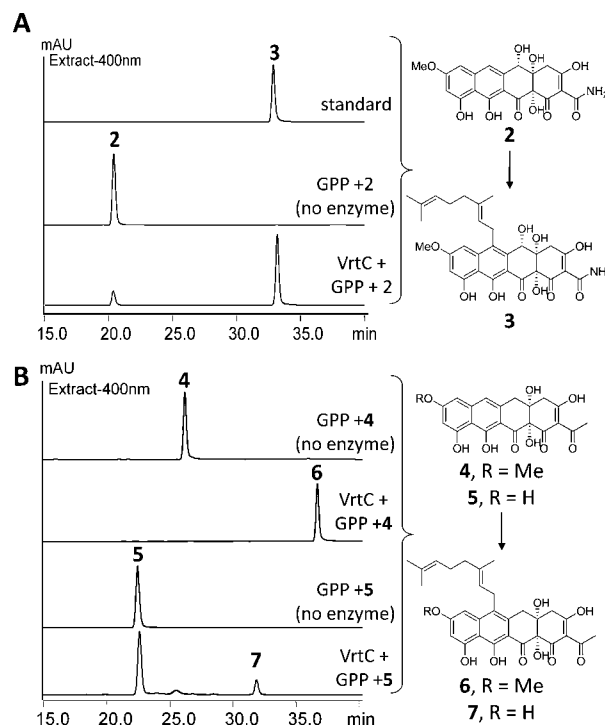

Figure 2. In vitro assays of VrtC. (A) HPLC analysis of VrtC in reaction with **2** and GPP comparing to the standard **3**. (B) HPLC analysis of VrtC reaction with **4** and **5**, and controls.
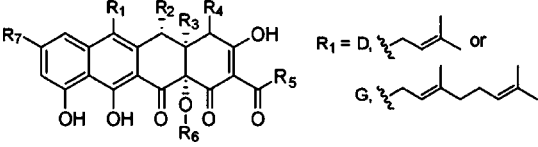
Δ*gsfA*/Δ*vrtC* mutant. Based on the calculated molecular weight and UV profile, **3** is likely to be the geranylated, uncyclized intermediate of **1** (Scheme 2). Compound **3** was isolated from 3-day stationary cultures of *P. aethiopicum* Δ*gsfA* strain grown on YMEG medium. Based on the ¹H, ¹³C, and 2D NMR analyses (Table S4) and reference to the NMR spectra of **1** and hypomycetin (Scheme 1),[21] the structure of **3** was assigned to be the C6-geranyl derivative of **2** and was named previridicatumtoxin as a late precursor to **1** (Scheme 2). Altogether, the loss of **1** and **3** accompanied with the accumulation of **2** in *P. aethiopicum* Δ*gsfA*/Δ*vrtC* mutant established that VrtC is the PTase in the *vrt* pathway.

In contrast to *vrtC*, deletion of *vrtD* did not abolish the production of **1**, but led to a significantly reduced titer. Furthermore, a substantial accumulation of the intermediate **2** in the culture of Δ*vrtD* can be observed. The accumulation of **2** could be due to insufficient supply of the geranyl diphosphate (GPP) substrate and is in agreement with the proposed function of VrtD as a GPPS, but not as a terpene cyclase (Scheme 2). Since an additional VrtD homologue is present in the *P. aethiopicum*,[18] the function of VrtD is likely to specifically supplement the GPP pool for biosynthesis of **1**. The clustering of *vrtD* in the *vrt* gene cluster suggests that it is likely to be co-regulated with other genes in the *vrt* pathway to ensure a synchronized supply of GPP during the production of **1**.

Reconstitution and Characterization of VrtC Activity. The coding region of *vrtC* was cloned into pET-28a expression vector and fused with an *N*-terminal His₆-tag. Soluble VrtC (calculated MW 53 kDa) was obtained from the *E. coli* BL21(DE3) and purified with Ni-NTA to apparent homogeneity as judged by SDS-PAGE (Figure S2A). Using inductively coupled optical emission spectroscopy (ICP-OES), it was determined that no significant amount of Ca^{2+}, Mg^{2+}, or Mn^{2+} ions is bound to VrtC (Table S5). To reconstitute the activity of VrtC, the purified enzyme was incubated with 0.5 mM GPP and 0.5 mM **2** in 50 mM Tris-HCl buffer. Nearly complete conversion of **2** to **3** can be observed by LC/MS (Figure 2A). The metal ion requirement of VrtC was tested by performing the prenylation reaction in the presence of 5 mM $CaCl_2$, $MgCl_2$, $MnCl_2$, $ZnCl_2$, or EDTA. Similar to other characterized fungal indole PTases, VrtC does not require any divalent ion to catalyze the geranyl transfer to **2**, and the addition of 5 mM EDTA did not reduce its activity significantly (Figure S2B). In the presence of Mn^{2+}, the activity of VrtC was increased by about 1.5-fold, but the presence of Zn^{2+} has an inhibitory effect on the reaction (Figure S2B). The kinetic parameters of the geranyl transfer reaction were measured in the presence of 5 mM Mn^{2+}. The K_M values for GPP and **2** were determined to

be 12.3 and 15.4 μM, respectively (Figure S2C). The k_{cat} of the reaction was calculated to be 1.42 min⁻¹.

The substrate specificity of VrtC toward different prenyl and polycyclic substrates were assayed. VrtC is specific to GPP and cannot catalyze the transfer of dimethylallyl to **2**. Besides **2**, VrtC was also tested with acetyl-primed tetracyclic compound TAN-1612 (2-acetyl-2-decarboxamido-anthrotainin, ADA) **4** and the *O*-desmethyl derivative **5** produced by the *ada* pathway in *Aspergillus niger* (Figure 2B).[19] VrtC was able to transfer a geranyl group successfully to both **4** and **5**, converting them to **6** (m/z 551 [M+H]⁺) and **7** (m/z 537 [M+H]⁺) respectively (Figures 2B and S4), but at a lower initial velocity than the native substrate **2** (Table 1). The conversion rate of **5** to **7** is also significantly slower than that of **4** to **6** (Figure 2B and Table 1), which implies the preference of VrtC toward the 8-*O*-methyl group present in **4** and **2**.

Geranyl transfer to bacterial tetracycline derivatives, such as the structurally similar 6-desmethyl-ATC obtained from our previous study of oxytetracycline pathway,[25] and the intermediate **11** [6-desmethyl-4a-hydroxy-4-des-(dimethylamino)anhydrotetracycline] of the SF2575 pathway (Table S7),[26] were unsuccessful. Similarly, tricyclic compounds such as emodin, norlichexanthone, and 3,6,8,9-tetrahydroxy-3-(2-oxopropyl)-3,4-dihydroanthracenone are not substrates for VrtC. Recently, the ABBA-type PTases from several fungal genomes have been shown to transfer a dimethylallyl group to the C3 position of 2,7-dihydroxynapthalene.[27] Hence, several dihydroxynaphthalene isomers, including the 2,7-dihydroxynaphthalene, were also tested as potential substrates, but none of these bicyclic substrate can be utilized by VrtC. Hence, VrtC appears to be highly selective toward tetracyclic naphthacenedione substrates.

Genome Mining of Fungal Polycyclic Aromatic PTases. The characterization of VrtC as a naphthacenedione

Table 1. Prenylated Compounds Generated in This Study and Relative Initial Velocities (V_{rel}) of the Prenylation Reactions Catalyzed by the pcPTases in Vitro[a]

substrate	product	R_1	R_2	R_3	R_4	R_5	R_6	R_7	pcPTase	V_{rel} (%)
2	3	G	OH	OH	H	NH_2	H	OCH_3	VrtC	100 ± 9.0
2	8	D	OH	OH	H	NH_2	H	OCH_3	Nf112230	27 ± 2.9
									Mc03599	19 ± 2.4
									Tt06703	11 ± 1.6
4	6	G	H	OH	H	CH_3	H	OCH_3	VrtC	73 ± 3.0
4	9	D	H	OH	H	CH_3	H	OCH_3	Nf112230	228 ± 4.2
									Mc03599	125 ± 3.0
									Tt06703	111 ± 3.1
5	7	G	H	OH	H	CH_3	H	OH	VrtC	37 ± 4.0
5	10	D	H	OH	H	CH_3	H	OH	Nf112230	87 ± 2.0
									Mc03599	240 ± 7.9
									Tt06703	366 ± 22.0
11	12	D	H	H	OH	NH_2	CH_3	H	Mc03599	N.D.
									Tt06703	

[a]Structures of **2**, **3**, **9**, and **11** were solved by NMR (Table S3−4 and S6−7); **4** and **5** were characterized in previous study;[19] the position of R_1 on **8**, **6**, **7**, **10**, and **12** was inferred on the basis of the structures of **3** and **9**. N.D. = not determined. Note that chain length specificities toward the isoprenoid substrates are orthogonal between VrtC (G) and the trio of genome-mined pcPTases (D).
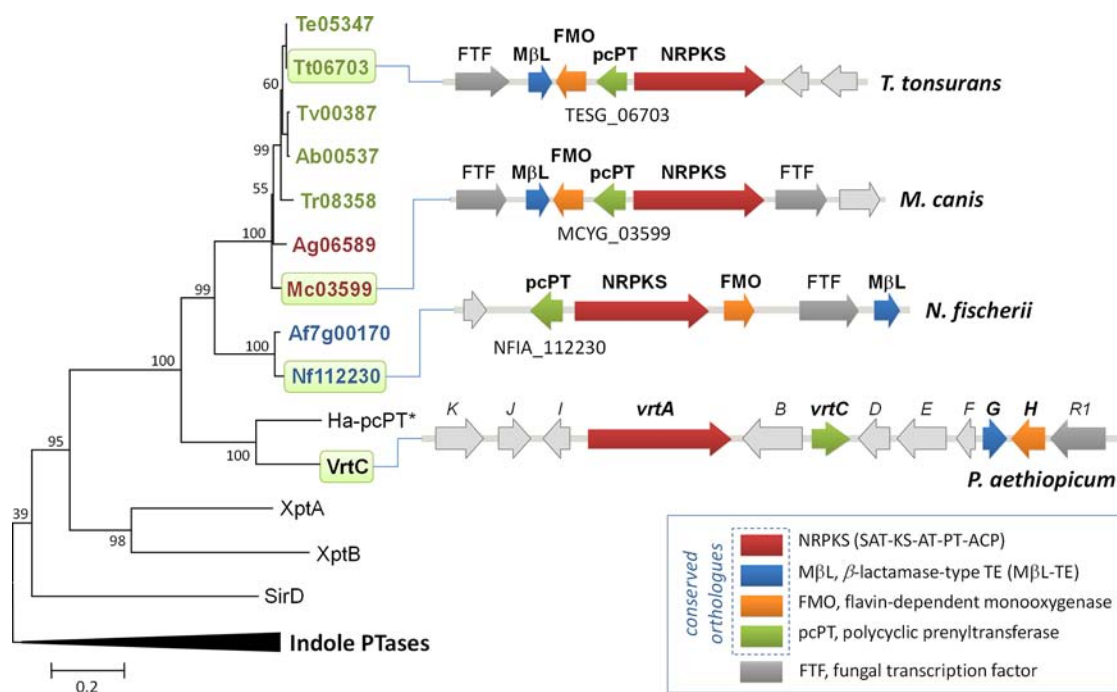

Figure 3. Phylogenetic relationship among the polycyclic PTases (pcPTases) and other DMATS-type PTases. The *vrt* cluster and the gene clusters associated to the pcPTases in, *N. fischeri* (Nf/NFIA), *M. canis* (Mc/MCYG) and *T. tonsurans* (Tt/TESG) are shown. The NRPKS/MβL-TE/FMO/pcPTase tetrads are orthologous genes conserved among the pcPTase-containing gene clusters. *Ha-pcPT only contained partial sequence. The prefixes of the gene IDs are abbreviated to two letters: Af, *A. fumigatus* (AFUA); Ag, *A. gypseum* (MGYG); Ab, *A. benhamiae* (ARB); Mc, *M. canis* (MCYG); Te, *T. equinum* (TEQG); Tr, *T. rubrum* (TERG); Tv, *T. verrucosum* (TRV), Ha, *H. aurantius*. An expanded phylogenetic tree is shown in Figure S5.
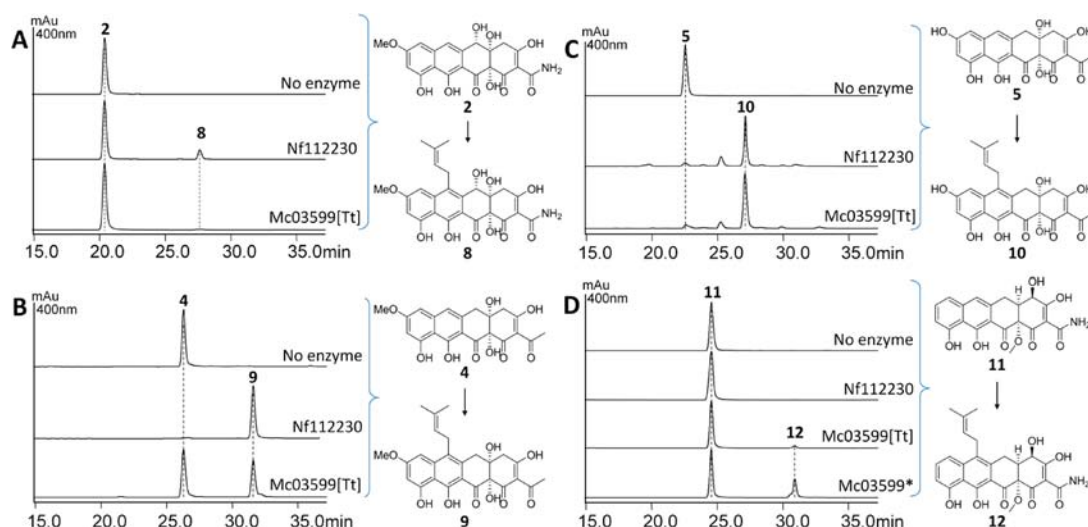
Figure 4. In vitro assays of pcPTases with DMAPP and naphthacenedione substrates showing conversion of (A) **2** to **8**, (B) **4** to **9**, (C) **5** to **10**, and (D) **11** to **12**. Assays are carried out for 4 h with 5 μM final concentration of corresponding enzyme, except (*) 25 μM Mc03599 was used to convert substrate **11** to **12** to generate a more prominent peak detectable by ESI-MS. Assays of Tt06703 [Tt] resulted in similar HPLC traces as Mc03599. The mass spectra of the products are shown in Figure S4.

geranyl transferase prompted us to search other sequenced fungal genomes in the public databases for potential PTases that could catalyze prenylation of linearly fused polycyclic substrates. BLASTP search of the GenBank, JGI, and Broad-MIT fungal genome databases identified nine PTases that exhibit considerable similarity (>40% protein identity) to VrtC. The nine PTases correspond to *Neosartorya fischeri* NFIA_112230, *Aspergillus fumigatus* AFUA_7G00170, *Microsporum canis* MCYG_03599, *Microsporum gypseum* MGYG_06589, *Trichophyton tonsurans* TESG_06703, *Trichophyton equinum* TEQG_05347, *Trichophyton rubrum* TERG_08358, *Arthroderma benhamiae* ARB_00537, and *Trichophyton verrucosom* TRV_00387. Interestingly, all of these VrtC homologues are found primarily in pathogenic fungi known to be associated with human or animal diseases, which include the closely related *A. fumigatus* and *N. fischeri*,[28] and the more recently sequenced group of arthrodermataceous dermatophytic fungi.[29] Phylogenetic analysis indicates that the VrtC-like PTases formed a separate clade from the indole PTases and the recently identified xanthone PTases from *A. nidulans* (Figures 3 and S5).[20] Furthermore, homologues of the three genes (NRPKS, *vrtA*; MβL-TE, *vrtG*; FMO, *vrtH*) essential for the biosynthesis of naphthacenedione structure,[19] are also present in vicinity of these VrtC-like PTase genes (Figure 3). A comparison of these orthologous genes to those in the *vrt* pathway and *ada* pathway is shown in Table S6. This hints that these newly identified VrtC homologues may catalyze a similar prenyl transfer reaction on a polyketide-derived polycyclic scaffold. Tentatively, we assigned this group of potential polycyclic aromatic PTases as "pcPTases".

The anti-fungal hypomycetin (Scheme 1) from *H. aurantius* contains a dimethylallyl group at the same C6 position of the naphthacenedione core as **3**. We reasoned that a similar PTase may responsible for the prenylation in the hypomycetin pathway. Blocks of conserved regions identified in the multiple sequence alignment were used in the design of degenerate primers pcPT-F and pcPT-R (Table S1), which were used to amplify a partial region of Ha-pcPT gene from *H. aurantius* (deposited in GenBank as JQ655772). As expected, Ha-pcPT clustered together with other pcPTases on the phylogenetic

tree and is likely to be the pcPTase involved in hypomycetin biosynthesis (Figure 3).

Expression, Purification, and in Vitro Assays of pcPTases. Further *in silico* analysis shown that besides the four homologous genes (NRPKS/MβL-TE/FMO/pcPTase), additional accessory genes can be found in vicinity of some of these gene clusters (Figure 3). Based on gene cluster composition and gene synteny, these nine gene clusters can be further divided roughly into three subgroups (Figure 3). A pcPTase from each subgroup, *N. fischeri* Nf112230 (NFIA_112230), *M. canis* Mc03599 (MCYG_03599), and *T. tonsurans* Tt06703 (TESG_06703), was selected for biochemical analysis. The three pcPTases were expressed and purified from *E. coli* as described for VrtC (Figure S3).

In vitro assays of the pcPTases with tetracyclic substrates (**2**, **4**, and **5**) showed that these enzymes utilize DMAPP instead of GPP as the prenyl donor. Nf112230 can convert the carboxamide-containing **2** to a new compound detectable by LC/MS with m/z 482 [M+H−H$_2$O]$^+$ and 500 [M+H]$^+$, which corresponds to the molecular weight expected for **8**, the C$_5$-prenylated derivative of **2** (Figures 4A and S4). Mc03599 and Tt06703 also appeared to convert a small amount of **2** to **8** albeit at a much lower relative velocities (Table 1). All three pcPTases can convert the acetyl-primed **4** to a corresponding C$_5$-prenylated product **9** with the expected m/z 483 [M+H]$^+$ (Figures 4B and S4). The relative initial conversion rate **4** to **9** by Nf112230 is about 2-fold faster than by Mc03599 and Tt06703 (Table 1). Besides **4**, all three pcPTases can transfer a dimethylallyl group to **5**, converting it to **10** with the expected m/z 469 [M+H]$^+$ (Figures 4C and S4). Mc03599 and Tt6703 appear to convert **5** to **10** at initial rates that are 2−3 times faster than for **4** to **9** (Table 1), indicating their preference toward substrates with an unmethylated C8 hydroxyl group. Nf112230, Mc03599, and Tt06703 were also tested for their ability to catalyze transfer of prenyl group to tetracycline derivatives of bacterial origins. Like VrtC, none of the three pcPTases can utilize 6-desmethyl-ATC as substrate. However, **11** can be prenylated by Mc03599 and Tt06703 to produce **12** with m/z 468 [M+H]$^+$ and 466 [M−H]$^−$, albeit with significant lower conversion (Figure 4D and S4). This indicates that

Mc03599 and Tt06703 may be less sensitive toward the hydroxyl at C4 and the absence of *O*-substitution at C8 compared to Nf112230 and VrtC. Taken together, it can be concluded that all three genome-mined pcPTases are dimethylallyl transferases instead of geranyl transferases and can utilize tetracyclic substrates as predicted from the phylogenetic analysis. The three enzymes displayed differences in substrate selectivity (especially C2 carboxamide and C8 methoxy), likely reflecting differences in their natural substrates in the respective fungal hosts.

Biotransformation of 4 in *E. coli* Expressing Nf112230. To confirm the putative regioselectivity of the newly identified pcPTases, **9** was produced via biotransformation of **4** in *E. coli* BL21(DE3) expressing Nf112230. A total of 10 mg/L of **4** was added to the culture 4 h after IPTG induction followed by shaking at 28 °C. Aliquots (2 mL) were sampled from the culture and analyzed by LC/MS after 20 and 48 h (Figure 5).
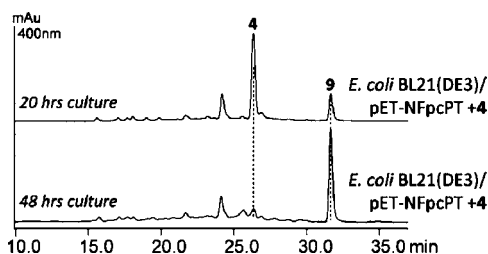

Figure 5. Biotransformation of **4** to **9** using *E. coli* BL21(DE3) culture expressing Nf112230 (pET-NFpcPT).

Nearly all of compound **4** appeared to have been converted to **9** after 3 days. Compound **9** was purified from the *E. coli* extracts by using a Sephadex-LH20 column and was subjected to extensive NMR analysis. The $^1H-^{13}C$ HMBC experiment, especially the correlation of C15 methylene protons to carbons C5a/C6/C6a, indicates that the geranyl group of **9** is installed at position C6 (Table S8). Most of the ^1H and ^{13}C NMR peaks are similar to the published NMR data of hypomycetin,[21] except for the methylene protons assigned to the position C5. This confirmed the structure of **9** as the 5-dehydroxy derivative of hypomycetin (Table S8). Since Mc03599 and Tt06703 yielded the same product **9** as Nf112230, the regioselectivity toward the C6 position is identical for these pcPTases. It can also be inferred that the positions of the dimethylallyl groups in **8**, **9** and **12** (products from **2**, **4**, and **11**) are at C6 as well (Table 1).

Anti-microbial Activities of the Prenylated and Non-prenylated Fused Ring Polyketides. We tested the prenylated and non-prenylated tetracyclic compounds that can be isolated in sufficient quantities for anti-bacterial and anti-yeast activities (Table 2). **1** has been previously reported to exhibit anti-MRSA activity,[17] and a study shows that the mechanism of action of **1** may be the inhibition of undecaprenyl pyrophosphate synthase (UPPS) involved in cell wall synthesis.[30] In this study, it is shown that **3** and **2** that lack the spirobicyclic ring retain almost the same anti-bacterial activity as **1** in the *Staphylococcus aureus* strain tested, while exhibiting higher minimal inhibitory concentration (MIC) for *Bacillus subtilis* than **1**. The additional geranyl group in **3** does not improve the activity compared to **2**, while the spirobicyclic ring of **1** appears to improve the inhibitory effect on *B. subtilis* and yeasts. The acetyl-primed **4** has not been reported to possess anti-bacterial activity but is known to act as

Table 2. Anti-bacterial and Anti-yeast Activities of Compounds Isolated in This Study[a]

compd	*Sa*	*Se*	*Bs*	*Ec*	*Ca*	*Sc*
1	0.125	>64	0.5	>64	4	4
2	0.125	>64	1	>64	32	32
3	0.125	>64	1	>64	32	32
4	16	>64	16	>64	>64	>64
9	0.5	>64	2	>64	>64	>64
ATC	0.5	8	0.5	8	32	32

[a]Minimal inhibitory concentration (MIC) values in μg/mL are shown. *Sa*, *S. aureus*; *Se*, *S. enterica*; *Ec*, *E. coli*; *Ca*, *C. albicans*; *Sc*, *S. cerevisiae*.

neuropeptide Y and neurokinin-1 receptor antagonists. The anti-bacterial activity of **4** on the gram-positive *S. aureus* and *B. subtilis* is markedly lowered compared to the carboxamide-containing **2**. This shows that either the carboxamide or the 5-hydroxy group in **2** is critical for the anti-bacterial activity. Interestingly, addition of dimethylallyl group to **4** (compound **9**) led to an increase in the anti-bacterial activity against both Gram-positive strains tested, albeit the MIC value is still higher than for **1**−**3**. All of the compounds tested did not inhibit the Gram-negative bacteria *E. coli* and *Salmonella enterica*. Besides **1**, none of the compounds has significant anti-yeast activity against *Saccharomyces cerevisiae* and *Candida albicans* (Table 2).

■ DISCUSSION

In this study, the role of VrtC in biosynthesis of **1** has been confirmed unequivocally by gene deletion, characterization of the blocked intermediate **2**, and reconstitution of the activity of VrtC in vitro. VrtC was shown to catalyze a regiospecific Friedel−Crafts alkylation of the naphthacenedione carboxamide substrate **2** at C6 using GPP as the prenyl donor substrate. VrtC exhibits moderate homology to the well-studied indole PTases (~25% identity) and contains the DMATS-type aromatic PTase superfamily conserved domain (cl15444) based on NCBI Conserved Domain-Search, and is thus a member of the DMATS-type PTases. Recently, VrtC has been included in a hidden-Markov Model-based analysis and was shown to be evolutionary related to the known indole PTases.[31] Therefore, VrtC is likely to contain a similar β/α barrel fold (PT fold) to the two structurally characterized indole PTases.[14,32] A homology model of VrtC with a PT fold based on FgaPT2 template is shown in Figure S7. Like all biochemically characterized DMATS-type PTases, VrtC is a soluble protein and its catalytic activity is not metal ion-dependent (Figure S2B). This is in agreement with the ICP-OES results, where none of the Ca^{2+}, Mg^{2+}, or Mn^{2+} ions was shown to be bound to VrtC (Table S5). Although metal ions are not essential, different divalent ions are known to enhance or inhibit the activity of these PTases, with each of the enzyme characterized so far has a slightly different profile.[10] For VrtC, the addition of Mn^{2+} resulted in the highest activity among the divalent ions tested followed by Ca^{2+}, while Zn^{2+} inhibits the enzyme activity.

So far, all the characterized fungal DMATS-type PTases, including the recently studied xanthone PTases (XptA and XptB) from *A. nidulans*, are only known to utilize DMAPP as prenyl donor. Most of the fungal aromatic PTases that were linked to the transfer of longer chain prenyl group, such as PaxC in paxiline pathway (C_{20}),[33] Pyr6 in pyripyropene pathway (C_{15}),[34] and MpaA in mycophenolic acid pathway (C_{15}),[35] are all belong to the membrane-associated PTases similar to UbiA and Coq2 in ubiquinone biosynthesis and

contain a characteristic (N/D)DXXD Mg^{2+}-diphosphate binding motif.[31] Thus, the ability to utilize GPP by the free VrtC is unique among DMATS-type PTases and suggests that the DMATS-type PTases can be evolved to transfer longer prenyl substrates.

The characterization of VrtC as a geranyl transferase that utilizes a unique ATC-like substrate prompted us to search for similar enzymes by genome mining, which uncovered nine highly homologous genes distributed among *A. fumigatus*, *N. fischeri*, and seven recently sequenced dermatophytes of the family Arthrodermataceae. This new subgroup of DMATS-type PTases exhibits lower protein similarity to the known fungal indole PTases (≤25% protein identity) and formed a separate distinct clade with VrtC in phylogenetic analysis (Figures 3 and S5). Interestingly, genes homologous to the *vrt*,[18] *ada*,[19] and *apt*[36] pathways encoding for NRPKS (homologous to VrtA/AdaA/AptA), MβL-TE (homologous to VrtG/AdaB/AptB), and FMO (homologous to VrtH/AdaC/AptC) are also found in vicinity of these VrtC homologues (pcPTases). Although the synteny of these gene clusters do not appear to be conserved (Figure 3), the high homology of the gene sets suggests a common ancestral origin and that they are likely encode for production of prenylated linear fused polycyclic metabolites (Table S6). This motivated us to further characterize these potentially tetracyclic-modifying PTases. As expected, all the three recombinant pcPTases (Nf112230, Mc03599, and Tt06703) were able to utilize the tetracyclic substrate **4** and **5**, but have different selectivity toward **2** and **11**. This successfully demonstrated that the specificity of PTases toward polycyclic aromatic substrates can be predicted from primary sequence information.

Equipped with these recombinant pcPTases and various naphthacenedione substrates, a total of seven C_5- or C_{10}-prenylated compounds were successfully synthesized, demonstrating their potential application in modification of pharmaceutically relevant scaffolds. Surprisingly, unlike VrtC, all three recombinant pcPTases (Nf112230, Mc03599, and Tt06703) appear to only utilize the shorter DMAPP and not GPP as the prenyl donor. This prenyl donor specificity is likely applicable to the other six pcPTases due to their high protein sequence similarity to Nf112230, Mc03599, and Tt06703. Ha-pcPT, despite sharing the highest protein similarity to VrtC among the pcPTases, is likely to utilize DMAPP as well, as evident in the structure of hypomycetin. We noticed that, Nf112230 appears to catalyze the prenylation of **4** and **5** at a much faster rate than **2** under the identical reaction condition. The initial conversation rate from **4** to **9** is about 8-fold faster than from **2** to **8** by Nf112230 (Table S1). The slower conversion of **2** by Nf112230 and the inability to utilize **2** by Mc03599 and Tt06703 could be due to the substrate specificity of the PTases toward the carboxamide group and/or the C5-hydroxyl group on **2**. This is not unexpected, since the native substrate of the three pcPTases are likely acetyl-primed and has no hydroxyl group at the C5 position due to lack of the genes required for the unique malonamyl starter unit biosynthesis (proposed to be *vrtJ* and *vrtB* in pathway of **1**) and a corresponding P450 hydroxylase homologue in all of the corresponding gene clusters. The ability of Nf112230, Mc03599, and Tt06703 to convert **4** to **9** (5-dehydroxyhypomycetin) demonstrates the possibility to reconstitute the pathway of hypomycetin without the genetic information in *H. aurantius*. Prenylation of aromatic compounds by biotransformation has previously been demonstrated using yeast

expressing plant membrane-bound PTase,[37] but it has not been shown in *E. coli* expressing DMATS-type PTases. The successful biotransformation of **4** to **9** in *E. coli* expressing Nf112230 shows the potential application of this approach in prenyl modification of pharmacologically relevant molecules and circumvents the use of expensive prenyl diphosphate substrates in enzymatic conversion. *E. coli* strains, engineered to produce higher titer of DMAPP or GPP substrates,[38] will be useful for such application.

The tetracycline family of antibiotics, which inhibits bacterial growth by interfering protein synthesis at ribosomal level, is widely used in human and animals. Based on the crystal structure of the tetracycline-bound 30S subunit ribosome, the "western" faces (corresponds to position C4−C9) of tetracyclines has been suggested as potential sites for modification to improve potency and to evade bacterial resistance.[39,40] Since VrtC and its homologues can catalyze prenylation at the C6 position of naphthacenedione substrates like **2** and **4**, we tested if these PTases could utilize naphthacenedione substrates that are more closely resembles the intermediates in the tetracycline pathway. These prenylated naphthacenedione compounds may be then further modified by enzymes downstream of the tetracycline pathway. 6-Desmethyl-ATC, lacking the methyl group at the C6 position obtained from our previous study of the oxytetracycline pathway,[25] was first tested, but none of the PTases including VrtC can accept this substrate. Interestingly, Mc03599 and Tt06703 can utilize **11**, a blocked intermediate from the anti-cancer tetracycline SF2575 pathway, and convert it to **12**. Compared to 6-desmethyl-ATC, **11** lacks the dimethylamino group at the C4 position and is replaced with a hydroxyl group. This indicates that the tested PTases are sensitive to the modification at this position and the dimethylamino group may be too large for the substrate cavity. Although the yield for conversion of **11** to **12** is low (thus hampering the structural characterization of **12**), the ability of Mc03599 and Tt06703 to utilize **11** is significant, as these two enzymes can be potential starting point for protein engineering to generate biocatalysts optimized for modification of various tetracycline scaffolds. Since the reactivity at the C6 position of such naphthacenedione systems is likely the most reactive site for Friedel−Crafts alkylation based on the electronics of the ring system, it is possible that similar modification can be achieved chemically though it has not been demonstrated.

The first protein crystal structure of a fungal DMATS-type PTase, *A. fumigatus* FgaPT2, has previously been solved.[14] The complex of FgaPT2 with L-tryptophan and dimethylallyl S-thiolodiphosphate (DMSPP) allowed us to mapped out the active-site residues involved in substrate interactions.[14] The residues involved in pyrophosphate binding in FgaPT2 [R100, K187, Y189, R257, K259, Y409, Y413 (numbering according to FgaPT2)] are reported to be conserved among the characterized fungal indole PTases.[14] Interestingly, multiple protein sequence alignment of pcPTases with FgaPT2 (Figure S6) showed that, except R100, R257, K259, and Y413, the other residues are not all conserved among VrtC and pcPTases. For example, the FgaPT2 Y409, which was shown to form a hydrogen bond with the terminal phosphate group of DMSPP, is replaced with an aspartate in all pcPTases as well as in *A. nidulans* XptA and XptB. This suggests that positioning of the pyrophosphate moiety in these polyketide PTases is likely to be different from that in indole PTases. The conserved E89 among indole PTases that interacts with the indole N−H and other

residues involved in L-tryptophan binding is deviated in the pcPTases as well. The corresponding E89 residue is replaced with a glycine in VrtC/Ha-pcPT and an asparagine in Nf112230/Af7g00170 and the seven pcPTases from arthrodermacetous fungi. Like E89 in FgaPT2, this asparagine or glycine residue may play a role in substrate binding in pcPTases, and the difference may reflect their selectivity toward different prenyl acceptor substrates. Protein crystal structures will be required to fully understand the structural basis for the prenyl donor and acceptor specificities of pcPTases, and will facilitate protein engineering of these enzymes.

The presence of these homologous NRPKS/MβL-TE/FMO/pcPTase gene sets primarily among the human or animal-associated fungi is intriguing as it suggests that these homologous gene clusters may provide a common ecological advantage to these opportunistic pathogenic fungi. However, no prenylated linear fused polycyclic metabolite has been reported from *A. fumigatus* and *N. fischeri*. The secondary metabolites from *A. fumigatus* are especially well-studied and thoroughly catalogued.[41] We have also cultured the *N. fischeri* strain in different media and culture conditions but have not detected any of the expected metabolites. Thus, the gene clusters in *A. fumigatus* and *N. fischeri* are likely to be silent. On the other hand, little is known about the secondary metabolites from arthrodermataceous fungi. Interestingly, reverse yellow pigmentation is commonly observed among the dermatophytic fungi belonging to the genera *Microsporum* and *Trichophyton* cultured on agar plates (e.g., *M. canis* on potato dextrose agar).[42] To our knowledge, the compound responsible for the yellow pigmentation in these fungi has not been identified and may be related to the prenylated polycyclic polyketides as **1**, **9**, and hypomycetin all exhibit bright yellow color. Similar reverse yellow pigmentation is also observed in the *H. aurantius* producing hypomycetin and in *P. aethiopicum* producing **1**. The prenylated polycyclic metabolites encoded in the genome of these pathogenic fungi warrant further investigations.

■ CONCLUSION

In conclusion, this study identified a new subgroup of DMATS-type PTases that are capable of catalyzing a Friedel−Crafts alkylation of naphthacenedione substrates with GPP or DMAPP at the C6 position. The discovery and characterization of this new group of polycyclic aromatic PTases (pcPTases) open up new opportunities to modify naphthacenedione and other similar linearly fused polycyclic systems, which have long been a pharmacologically significant scaffold. We demonstrated that the PTase substrate specificity can be predicted on the basis of primary sequence information. The sequence information established in this study will be useful for genome mining of other prenylated polyketide pathways in fungi.

■ MATERIALS AND METHODS

Strains and Culture Conditions. *P. aethiopicum* IBT 5753 was obtained from the IBT culture collection (Kgs. Lyngby, Denmark) and maintained on YMEG agar (4 g/L yeast extract, 10 g/L malt extract, and 16 g/L agar) or GMM at 30 °C. *P. aethiopicum* ΔgsfA::zeo^R, which was blocked in griseofulvin biosynthesis, was obtained from a previous study.[23] *N. fischeri* NRRL 181 was obtained from ARS (NRRL) culture collection (Peoria, IL) and maintained on potato dextrose agar (Difco). The *E. coli* strains XL-1 Blue (Stratagene) and TOPO10 (Invitrogen) were used for DNA manipulation, and BL21(DE3) (Stratagene) was used for protein expression. *H. aurantius* CBS 276.65 was obtained from Centraalbureau voor Schimmelculturen (CBS),

Netherlands. *A. fumigatus* Af293 was obtained from Fungal Genetics Stock Center (FGSC, Kansas City, MO).

General Techniques for DNA Manipulation. Genomic DNA from *P. aethiopicum* and *N. fischeri* was prepared using the CTAB isolation buffer as described elsewhere,[43] or using ZYMO ZR fungal/bacterial DNA kit (Zymo Research) according to the manufacturer's protocol. Genomic DNA from *M. canis* (*Athroderma otae*) and *T. tonsurans* was a kind gift from Prof. Theodore White at the School of Biological Sciences, University of Missouri−Kansas City. PCR reactions were performed with Phusion high-fidelity DNA polymerase (New England Biolabs) or Platinum Pfx DNA polymerase (Invitrogen). PCR products were subcloned into pCR-Blunt vector (Invitrogen) and confirmed by DNA sequencing. Primers used to amplify the genes were synthesized by Integrated DNA Technologies and are listed in Table S1.

Genetic Manipulation of *P. aethiopicum*. Deletion of vrtC and vrtD was accomplished by a double homologous gene replacement cassette containing the bar resistance marker generated by the fusion-PCR method described previously,[18,44] and the gene deletion strategy is illustrated in Figure S1. Transformation of *P. aethiopicum* was carried out using the polyethyelene-glycol method as described previously.[18] Diagnostic PCR was performed with miniprep genomic DNA from individual transformants prepared using a previously described method.[45] Primers used for the generation of gene deletion cassettes and diagnostic PCR are listed in Table S1.

In Silico Genomic Analysis. The VrtC translated protein sequence, as described in previous work,[18] was used for BLASTP query at the NCBI GenBank database (http://www.ncbi.nlm.nih.gov) and the Broad Institute-MIT Aspergillus and Dermatophyte comparative databases (http://www.broadinstitute.org/). The protein sequences used in phylogenetic analyses shown in Figure 3 are listed in Table S2. The Minimal Evolution method, embedded in the MEGA 5 program,[46] was used for the calculation of the phylogenetic tree with 500 bootstrap replicates. An expanded DMATS-type PTase phylogenetic tree is shown in Figure S5.

Overexpression and Purification of His6-Tagged PTases. All PTase genes investigated in this study are devoid of introns. Therefore, the open reading frames were directly PCR-amplified from the genomic DNA of the corresponding organisms and cloned into pET28a plasmid (Merck Biosciences). Primers used for the amplification and cloning are listed in Table S1. All the PTase proteins are expressed with N-terminal His6-tagged in *E. coli* BL21(DE3) and purified by nickel affinity chromatography. Briefly, the cells were cultured at 37 °C 250 rpm in 500 mL of LB medium with 35 μg/mL kanamycin. Next, 0.1 M isopropylthio-β-D-galactoside (IPTG) was added at OD_{600} = 0.4−0.6 and incubated for another for 12−16 h at 16 °C. The cells were then harvested by centrifugation (3500 rpm, 15 min, 4 °C), resuspended in ∼25 mL of lysis buffer (20 mM Tris-HCl, pH 7.9, 0.5 M NaCl, 10 mM imidazole), and lysed by sonication on ice. Cellular debris was removed by centrifugation (15 000 rpm, 30 min, 4 °C), and the His6-tagged proteins were purified from the supernatant by using Ni-NTA agarose (Qiagen) according to the manufacturer's instructions. The protein was eluted with 250 mM imidazole in buffer A (50 mM Tris-HCl 2 mM EDTA 2 mM DTT, pH 8.0). Finally, the purified protein was concentrated and exchanged into buffer A with 10% glycerol using Centriprep filters (Amicon) and stored at −80 °C for enzyme assays.

Assay for PTase Activity. All enzyme assays are performed in 50 mM Tris-HCl buffer, pH 7.5, at 30 °C. DMAPP and GPP used in the enzyme assays are from Echelon Biosciences. To terminate the PTase reaction, an equal volume of EtOAc/MeOH/AcOH (89:10:1) was added and vortexed vigorously. After centrifugation, the products of the enzymatic reaction were obtained from the top organic phase, and the extraction was repeated once, pooled, and dried for high-performance liquid chromatography (HPLC) or LC/MS analyses. To test the influence of different metal ions on VrtC activity, a 5 mM concentration of each divalent metal ions and EDTA are added to the enzyme assays with 0.5 mM GPP and **2**. The enzymatic reactions were allowed to proceed for 10 min. The assays for determination of the kinetic parameters of **2** for VrtC contained 5 mM MnCl2, 500 μM

GPP, 1 μg (200 nM) of VrtC, and **2** at a final concentration of 0, 10, 20, 50, 100, 200, or 500 μM in a total volume of 100 μL. For the kinetic parameters of GPP for VrtC, 5 mM $MnCl_2$, 500 mM **2**, 200 nM VrtC, and GPP at a final concentration of 0, 10, 20, 50, 100, 200, or 500 μM were used in the assays. For testing the activity of the VrtC homologues (pcPTases) with non-native naphthacenedione substrates, each of the enzymes was added to a final concentration of 1−5 μM and reacted with 0.5 mM DMAPP and 0.5 mM naphthacenedione substrate for up to 4 h.

Biotransformation in E. coli. Compound **4** (TAN-1612, 2-acetyl-2-decarboxamidoanthrotainin) was obtained from our previous study.[19] To obtain a sufficient amount of the prenylated product **9** for structural characterization, we used *E. coli* BL21(DE3) expressing the Nf112230 to convert the substrate **4** to **9**. The *E. coli* strain was grown in 2 L of Terrific Broth (TB) medium to OD_{600} = 0.6 at 37 °C, 250 rpm followed by induction of Nf112230 protein expression with 0.1 M IPTG. After additional 4 h of shaking incubation at 28 °C, 10 mg/L of substrate **4** was added to the culture, and it was grown for an additional 3 days at 28 °C. The culture was sampled (2 mL) at 24 and 48 h and extracted with EtOAc/MeOH/AcOH (89:10:1) for HPLC analysis to monitor the conversion of **4** to **9**.

Chemical Analyses. For HPLC analyses, the dried organic samples were dissolved in MeOH and analyzed with a Shimadzu LC-20AD system with a Phenomenex Luna 5 μm, 2.0 × 100 mm C18 reverse-phase column coupled to a Shimadzu SPD-M20A UV−vis detector. For LC/MS analyses, the liquid chromatographic system was coupled to a 2010 EV liquid chromatography mass spectrometer monitored with both positive and negative electrospray ionization. Most chromatographic separation was achieved with a linear gradient of 5% (v/v) solvent B (CH_3CN with 0.1% formic acid) to 95% solvent B over 30 min with a flow rate of 0.1 mL/min. For analyses of in vitro enzymatic products from kinetic assays, a shorter linear gradient of 30% to 95% solvent B over 15 min with a flow rate of 0.1 mL/min was used.

Compound Purification and Structural Characterization. Compound **2** is purified from $\Delta gsfA\Delta vrtC$ mutant strain cultured at stationary YMEG liquid medium (2 L) at 28 °C for 5 days. **3** was purified from $\Delta gsfA$ mutant strain grown at stationary YMEG liquid culture (4 L) at 28 °C for 2−3 days, as longer incubation reduces the compound **3** to **1** ratio. Compound **9** was purified from *E. coli* BL21 culture expressing Nf112230. All the initial extractions of organic compounds from culture were performed with equal volume of EtOAc/MeOH/AcOH (89:10:1), followed by crude separation using solvent partition with $CHCl_3/H_2O$ and hexane/90% MeOH. Isolation of the compounds was achieved by a combination of chromatographic separations on Sephadex LH-20 (GE Healthcare) column and preparative HPLC. More details on purification of each compound are provided in Supporting Information. All 1D and 2D NMR of **1** were performed on a Bruker DRX-500 or AV500 spectrometer. DMSO-d_6 was used as the solvent for all compounds except **9**, which used $CDCl_3$, as **9** is unstable in DMSO.

Anti-microbial Assays. For testing the anti-bacterial activities of the compounds, Gram-positive *S. aureus* and *B. subtilis*, and Gram-negative *S. enterica* serovar Cerro 87 and *E. coli* DH10B, were used. The *S. aureus*, *B. subtillis*, and *S. enterica* strains were obtained from Shanghai Jiao Tong University, China. The MIC assays were performed in 96-well plates in quadruplicates with the bacterial strains inoculated in LB broth at a starting OD_{600} = 0.00025 (diluted from cultures with OD_{600} = 0.4−1.0) and a series of 1:2 dilutions of the test compounds starting at 64 μg/mL to 0.03 μg/mL. The plates were incubated 24 h at 37 °C and visually inspected for growth inhibition. For anti-yeast assays, *S. cerevisiae* BY4741 and *C. albicans* ATCC 36082 were used. The *C. albicans* strain is a kind gift from Dr. Scott G. Filler at Harbor-UCLA Medical Center. The anti-yeast assays followed the broth microdilution method recommended by the Clinical and Laboratory Standards Institute.[47] The 96-well plates were incubated 48 h at 30 °C for *S. cerevisiae* and at 37 °C for *C. albicans*.

■ **ASSOCIATED CONTENT**

Ⓢ Supporting Information

NMR and MS characterization of compounds and additional experimental information including ICP-OES analysis. This material is available free of charge via the Internet at http://pubs.acs.org.

■ **AUTHOR INFORMATION**

Corresponding Author

yitang@ucla.edu; yhchooi@ucla.edu

Notes

The authors declare no competing financial interest.

■ **REFERENCES**

(1) Usui, T.; Kondoh, M.; Cui, C. B.; Mayumi, T.; Osada, H. *Biochem. J.* **1998**, *333*, 543.

(2) Woehlecke, H.; Osada, H.; Herrmann, A.; Lage, H. *Int. J. Cancer* **2003**, *107*, 721.

(3) Alt, S.; Mitchenall, L. A.; Maxwell, A.; Heide, L. *J. Antimicrob. Chemother.* **2011**, *66*, 2061.

(4) Sintchak, M. D.; Fleming, M. A.; Futer, O.; Raybuck, S. A.; Chambers, S. P.; Caron, P. R.; Murcko, M. A.; Wilson, K. P. *Cell* **1996**, *85*, 921.

(5) Erkel, G.; Anke, T.; Sterner, O. *Biochem. Biophys. Res. Commun.* **1996**, *226*, 214.

(6) Botta, B.; Vitali, A.; Menendez, P.; Misiti, D.; Monache, G. D. *Curr. Med. Chem.* **2005**, *12*, 713.

(7) Watjen, W.; Weber, N.; Lou, Y.; Wang, Z.; Chovolou, Y.; Kampkotter, A.; Kahl, R.; Proksch, P. *Food Chem. Toxicol.* **2007**, *45*, 119.

(8) Jain, H. D.; Zhang, C.; Zhou, S.; Zhou, H.; Ma, J.; Liu, X.; Liao, X.; Deveau, A. M.; Dieckhaus, C. M.; Johnson, M. A. *Biorg. Med. Chem.* **2008**, *16*, 4626.

(9) Botta, B.; Monache, G. D.; Menendez, P.; Boffi, A. *Trends Pharmacol. Sci.* **2005**, *26*, 606.

(10) Steffan, N.; Grundmann, A.; Yin, W. B.; Kremer, A.; Li, S. M. *Curr. Med. Chem.* **2009**, *16*, 218.

(11) Heide, L. *Curr. Opin. Chem. Biol.* **2009**, *13*, 171.

(12) Tello, M.; Kuzuyama, T.; Heide, L.; Noel, J.; Richard, S. *Cell. Mol. Life Sci.* **2008**, *65*, 1459.

(13) Kremer, A.; Li, S. M. *Microbiology* **2010**, *156*, 278.

(14) Metzger, U.; Schall, C.; Zocher, G.; Unsöld, I.; Stec, E.; Li, S. M.; Heide, L.; Stehle, T. *Proc. Natl. Acad. Sci. U.S.A.* **2009**, *106*, 14309.

(15) Hutchison, R.; Steyn, P.; Van Rensburg, S. *Toxicol. Appl. Pharmacol.* **1973**, *24*, 507.

(16) Raju, M.; Wu, G. S.; Gard, A.; Rosazza, J. *J. Nat. Prod.* **1982**, *45*, 321.

(17) Zheng, C. J.; Yu, H. E.; Kim, E. H.; Kim, W. G. *J. Antibiot.* **2008**, *61*, 633.

(18) Chooi, Y. H.; Cacho, R.; Tang, Y. *Chem. Biol.* **2010**, *17*, 483.

(19) Li, Y.; Chooi, Y.-H.; Sheng, Y.; Valentine, J. S.; Tang, Y. *J. Am. Chem. Soc.* **2011**, *133*, 15773.

9436

dx.doi.org/10.1021/ja3028636 | *J. Am. Chem. Soc.* 2012, 134, 9428−9437

(20) Sanchez, J. F.; Entwistle, R.; Hung, J. H.; Yaegashi, J.; Jain, S.; Chiang, Y. M.; Wang, C. C. C.; Oakley, B. R. *J. Am. Chem. Soc.* **2011**, *133*, 4010.

(21) Breinholt, J.; Jensen, G. W.; Kjær, A.; Olsen, C. E.; Rosendahl, C. N. *Acta Chem. Scand.* **1997**, *51*, 855.

(22) Lesburg, C. A.; Zhai, G.; Cane, D. E.; Christianson, D. W. *Science* **1997**, *277*, 1820.

(23) Gao, X.; Chooi, Y.-H.; Ames, B. D.; Wang, P.; Walsh, C. T.; Tang, Y. *J. Am. Chem. Soc.* **2011**, *133*, 2729.

(24) Wong, S.-M.; Kullnig, R.; Dedinas, J.; Appell, K. C.; Kydd, G. C.; Gillum, A. M.; Cooper, R.; Moore, R. *J. Antibiot.* **1993**, *46*, 214.

(25) Zhang, W.; Watanabe, K.; Cai, X.; Jung, M. E.; Tang, Y.; Zhan, J. *J. Am. Chem. Soc.* **2008**, *130*, 6068.

(26) Pickens, L. B.; Kim, W.; Wang, P.; Zhou, H.; Watanabe, K.; Gomi, S.; Tang, Y. *J. Am. Chem. Soc.* **2009**, *131*, 17677.

(27) Haug-Schifferdecker, E.; Arican, D.; Brückner, R.; Heide, L. *J. Biol. Chem.* **2010**, *285*, 16487.

(28) Nierman, W. C.; Pain, A.; Anderson, M. J.; Wortman, J. R.; Kim, H. S.; Arroyo, J.; Berriman, M.; Abe, K.; Archer, D. B.; Bermejo, C. *Nature* **2005**, *438*, 1151.

(29) Burmester, A.; Shelest, E.; Glöckner, G.; Heddergott, C.; Schindler, S.; Staib, P.; Heidel, A.; Felder, M.; Petzold, A.; Szafranski, K. *Genome Biol.* **2011**, *12*, R7.

(30) Inokoshi, J.; Nakamura, Y.; Zhang, H.; Uchida, R.; Masuma, R.; Omura, S.; Tomoda, H. *Drug Discov. Ther.* **2008**, 13.

(31) Bonitz, T.; Alva, V.; Saleh, O.; Lupas, A. N.; Heide, L. *PloS One* **2011**, *6*, e27336.

(32) Jost, M.; Zocher, G.; Tarcz, S.; Matuschek, M.; Xie, X.; Li, S. M.; Stehle, T. *J. Am. Chem. Soc.* **2010**, *132*, 17849.

(33) Young, C.; McMillan, L.; Telfer, E.; Scott, B. *Mol. Microbiol.* **2001**, *39*, 754.

(34) Itoh, T.; Tokunaga, K.; Matsuda, Y.; Fujii, I.; Abe, I.; Ebizuka, Y.; Kushiro, T. *Nat. Chem.* **2010**, *2*, 858.

(35) Regueira, T. B.; Kildegaard, K. R.; Hansen, B. G.; Mortensen, U. H.; Hertweck, C.; Nielsen, J. *Appl. Environ. Microbiol.* **2011**, *77*, 3035.

(36) Szewczyk, E.; Chiang, Y. M.; Oakley, C. E.; Davidson, A. D.; Wang, C. C. C.; Oakley, B. R. *Appl. Environ. Microbiol.* **2008**, *74*, 7607.

(37) Sasaki, K.; Tsurumaru, Y.; Yazaki, K. *Biosci., Biotechnol., Biochem.* **2009**, *73*, 759.

(38) Martin, V. J. J.; Pitera, D. J.; Withers, S. T.; Newman, J. D.; Keasling, J. D. *Nat. Biotechnol.* **2003**, *21*, 796.

(39) Khosla, C.; Tang, Y. *Science* **2005**, *308*, 367.

(40) Pioletti, M.; Schünzen, F.; Harms, J.; Zarivach, R.; Glühmann, M.; Avila, H.; Bashan, A.; Bartels, H.; Auerbach, T.; Jacobi, C. *EMBO J.* **2001**, *20*, 1829.

(41) Frisvad, J. C.; Rank, C.; Nielsen, K. F.; Larsen, T. O. *Med. Mycol.* **2008**, *47*, 53.

(42) Rebell, G.; Taplin, D. *Dermatophytes: their recognition and identification*; University of Miami Press, 1970.

(43) Carlson, J.; Tulsieram, L.; Glaubitz, J.; Luk, V.; Kauffeldt, C.; Rutledge, R. *Theor. Appl. Genet.* **1991**, *83*, 194.

(44) Szewczyk, E.; Nayak, T.; Oakley, C. E.; Edgerton, H.; Xiong, Y.; Taheri-Talesh, N.; Osmani, S. A.; Oakley, B. R. *Nature Protocols* **2007**, *1*, 3111.

(45) Chooi, Y.-H.; Stalker, D. M.; Davis, M. A.; Fujii, I.; Elix, J. A.; Louwhoff, S. H. J. J.; Lawrie, A. C. *Mycol. Res.* **2008**, *112*, 147.

(46) Tamura, K.; Peterson, D.; Peterson, N.; Stecher, G.; Nei, M.; Kumar, S. *Mol. Biol. Evol.* **2011**, *28*, 2731.

(47) Schwalbe, R. *Antimicrobial susceptibility testing protocols*; CRC, 2007.